

---

---

## ORIGINAL ARTICLE

---

---

# Influence of Susceptibility-weighted Imaging on Brain Magnetic Resonance Imaging Diagnostics

N Sanghan, V Charoonratana, S Hirunpat

Department of Radiology, Prince of Songkla University, Songkhla, Thailand

### ABSTRACT

**Objectives:** To evaluate the influence of susceptibility-weighted imaging (SWI) on detection rates and reported results in the diagnosis of various brain conditions, compared with conventional magnetic resonance imaging (MRI).

**Methods:** Brain MRI was obtained for various indications in 251 patients (115 male, 136 female). The mean age of the patients was 49.91 years. Two neuroradiologists independently evaluated the detection rates and reported results of brain MRI with and without SWI sequences. Statistical analysis was performed by using McNemar's Chi-square test and Cohen's kappa coefficient.

**Results:** Neuroradiologists 1 and 2 considered SWI to have influenced detection in 51% and 53% of patients, respectively, and to have influenced the reported results in 20% and 18% of patients, respectively. SWI had the strongest influence in the detection rates of vascular disease in 22 patients (100%) and calcification and abscesses in two patients (100%). SWI had the strongest influence on the reported results of vascular disease in 20 patients (91%) and of neurodegenerative / demyelinating in 11 patients (79%). There was excellent inter-observer reliability between neuroradiologists 1 and 2 (kappa value = 0.883-0.936).

**Conclusion:** SWI is a helpful technique in routine brain MRI sequences, and influences the detection rates and reported results, especially for vascular disease, microbleeds, infection, neurodegenerative / demyelinating disease, and evaluation of intratumoral components. SWI should be added to conventional MRI sequences.

**Key Words:** Brain; Magnetic resonance imaging

## 中文摘要

### 磁敏感加權成像對腦磁共振成像診斷的影響

N Sanghan、V Charoonratana、S Hirunpat

**目的：**與常規磁共振成像（MRI）相比，評估磁敏感加權成像（SWI）對檢測率和各種腦部疾病診斷報告結果的影響。

---

**Correspondence:** Dr N Sanghan, Department of Radiology, Prince of Songkla University, Songkhla, Thailand.

Email: [snuttha@medicine.psu.ac.th](mailto:snuttha@medicine.psu.ac.th)

Submitted: 5 May 2017; Accepted: 5 Jun 2017.

Disclosure of Conflicts of Interest: All authors have disclosed no conflicts of interest.

Funding/Support: This research received no specific grant from any funding agency in the public, commercial, or not-for-profit sectors.

Ethics Approval: This study was approved by the institutional review board of Songklanagarind Hospital (Research Ethics Committee [REC] Ref: 58-100-07-4). The institutional review board waived the requirement for patient consent for this retrospective study.

**方法：**選取251名患者（115名男性，136名女性）符合各種適應症的腦部MRI檢查。患者平均年齡為49.91歲。兩名神經放射學家獨立評估在有和沒有SWI序列下的腦部MRI檢測率和報告結果。研究使用McNemar卡方檢驗和Cohen kappa係數進行統計分析。

**結果：**第一名神經放射學家認為SWI對51%患者的檢測及20%患者的報告結果產生影響；第二名神經放射學家則認為SWI對53%患者的診斷及18%患者的報告結果產生影響。SWI對檢測血管疾病（22名患者，100%）及鈣化／膿腫（2名患者，100%）的影響最大。SWI對血管疾病（20名患者，91%）和神經退化／脫髓鞘（11名患者，79%）的報告結果影響最大。兩名神經放射學家的觀察者間信度極高（kappa值：0.883-0.936）。

**結論：**SWI是常規腦部MRI序列中的一種有用技術，可影響檢測率和報告結果，特別是血管疾病、微出血、感染、神經退化／脫髓鞘疾病及腫瘤內成分的評估。應將SWI加到常規MRI序列中。

## INTRODUCTION

Susceptibility-weighted imaging (SWI) is a phase-contrast enhancement imaging technique on magnetic resonance imaging (MRI). It offers information about any tissue that has a susceptibility that is different from the surrounding structures, such as deoxygenated blood, hemosiderin, ferritin, and calcium.<sup>1</sup> The local magnetic heterogeneity induced by paramagnetic, diamagnetic, and ferromagnetic substances can result in overall signal loss in gradient recalled echo (GRE) images and a de-phase change. The susceptibility effect is highest in GRE techniques at long echo times and high field strengths. The image contrast in magnitude images is acquired by using a high-resolution three-dimensional, fully velocity-compensated, T2\*-weighted GRE pulse sequence. Phase images are used to create a phase mask after unwrapping and high pass filtering. This phase mask is then multiplied with the magnitude images to enhance the visibility of small veins and other paramagnetic substances.<sup>2,3</sup> There are three components to SWI interpretation. First, the original magnitude images highlight susceptibility as signal intensity losses. Second, phase images express the phase differences of tissues. For a left-handed system, veins will look bright on the phase images owing to the paramagnetic effect of deoxygenated blood, and calcium will look dark because of its diamagnetic effect. Third, T2\*signal-intensity losses in the magnitude images are used to construct minimum intensity projection (MinIP) images for visualisation of the veins, similar to using maximum intensity projection (MIP) images to visualise arteries in MR angiography.<sup>1</sup>

Several studies have reported that SWI provides additional clinically useful information that is often complementary to conventional MRI sequences in the evaluation of various neurologic disorders,

including traumatic brain injury, stroke, intracranial haemorrhage, vascular malformations, neoplasms, and neurodegenerative disorders associated with intracranial calcification or iron deposition.

Since 2009, SWI—including magnitude, phase, and MinIP images—has been included in brain MRI evaluations in Songklanagarind Hospital, Songkhla, Thailand. However, it is time-consuming to scan and perform corrected phase imaging and MinIP imaging. The objectives of this study were to evaluate the influence of SWI on detection rates and reported results of brain MRI, to clarify whether adding SWI to routine imaging protocols is worthwhile.

## METHODS

### Patient Selection and Data Collection

This retrospective study was conducted at Songklanagarind Hospital. Patients were included who had undergone brain MRI with SWI sequence—including phase, magnitude, and MinIP images—from November 2014 to October 2015. Patients with incomplete SWI information were excluded. Patient demographic data, history of brain surgery and cranial radiation therapy, indication for performing MRI, and imaging manifestations were recorded.

### Imaging Acquisition

Two MRI machines with left-handed systems were used; one 1.5-T MRI machine (Ingenia; Philips, the Netherlands), and one 3-T MRI machine (Achieva X-series; Philips). Our routine brain protocol includes axial T1-weighted (T1W) imaging, T2-weighted (T2W) imaging, fluid attenuation inversion recovery (FLAIR) imaging, diffusion-weighted imaging, apparent diffusion coefficient, and GRE imaging; sagittal T1W imaging and

FLAIR imaging; and coronal T2W imaging. Gadolinium-based contrast administration depends on indications.

For SWI acquisition, the 1.5-T MRI imaging specifications were dStream (Philips), 15-channel head coil, gradient system, maximum gradient strength 45 mT/m, slew rate 200 T/m/s, repetition time 30 ms, echo time 45 ms, fractional anisotropy 15 degrees, pixel size 1.0 × 1.0 mm, slice thickness 1 mm, field of view 180 × 230 mm, acquisition time 258 s, SENSitivity Encoding factor 1.8, and 140 slices. The 3-T MRI imaging specifications were non-multitransmit type using an 8-channel SENSitivity Encoding head coil, Quasar Dual gradient system, maximum gradient strength 80 mT/m, slew rate 200 T/m/s, repetition time 15 ms, echo time 21 ms, fractional anisotropy 10 degrees, pixel size 1.0 × 0.99 mm, slice thickness 0.8 mm, field of view 200 × 240 mm, acquisition time 204 s, SENSitivity Encoding factor 1.3, and 170 slices.

### Imaging Analysis

Two experienced neuroradiologists independently interpreted and evaluated all brain MRI images. Radiologist 1 had 30 years of experience and radiologist 2 had 4 years of experience in neurological imaging. The two radiologists assessed whether SWI influenced detection rates for abnormalities, and whether SWI influenced the reported results.

All imaging diagnoses were classified into 10 groups: ischaemic stroke, tumour, vascular disease (vascular malformation and small vessel disease), neurodegenerative / demyelinating disease, infection, calcification, haemorrhage, normal study, inconclusive, and others (air, morning glory syndrome, lymphocytic hypophysitis, syringomyelia, von Hippel–Lindau syndrome, Chiari malformation, extracranial mass, Parry-Romberg syndrome, and colpocephaly).

### Statistical Analysis

Data were analysed using EpiData version 3.1. Chi-square test was used to assess the influence of SWI on each diagnostic categorisation. Inter-observer reliability was evaluated using Cohen's kappa coefficient. A kappa value of 0.01-0.2 indicated slight agreement, 0.21-0.4 indicated fair agreement, 0.41-0.6 indicated moderate agreement, 0.61-0.8 indicated good agreement, and 0.81-0.99 indicated excellent agreement.

## RESULTS

Brain MRI with SWI was obtained for various indications

in 251 patients (115 male, 136 female, mean age 49.91 years, range 1.25-85 years). Of these, 50 patients received 1.5-T MRI and 201 patients received 3-T MRI.

In all, 114 patients (45.4%) had a history of brain surgery and a few (1.2%) had undergone cranial radiation therapy. The most common indication to perform MRI was postoperative evaluation of brain tumours. Final diagnosis was selected from one of 10 categories (Table 1).

Neuroradiologists 1 and 2 considered that SWI had influenced the detection in 51% and 53% of patients, respectively, and that SWI had influenced the reported results in 20% and 18% of patients (Table 2). The strongest influences of SWI were on the detection rates and diagnosis of vascular disease (Figure 1), calcification (Figure 2), and infection (Figure 3). SWI had the strongest influence on reported results for vascular disease and neurodegenerative / demyelinating disease.

There was excellent agreement between neuroradiologists 1 and 2, with good inter-observer reliability (overall kappa value = 0.883-0.936) for all diagnostic categories.

## DISCUSSION

Most previous studies have focused on the ability of SWI to detect magnetic heterogeneity induced by paramagnetic, diamagnetic, and ferromagnetic substances present in various neurological disorders. The present study is concerned with the importance of more detectable findings and how they influence the final diagnosis or reported results.

**Table 1.** Final diagnosis after 1.5-T or 3-T magnetic resonance imaging.\*

Final diagnosis	1.5-T MRI (n=50)	3-T MRI (n=201)
Ischaemic stroke	2 (4.0%)	8 (4.0%)
Tumour	18 (36.0%)	82 (40.8%)
Vascular disease	5 (10.0%)	17 (8.5%)
Neurodegenerative / demyelinating disease	2 (4.0%)	12 (6.0%)
Infection	0	2 (1.0%)
Calcification	1 (2.0%)	1 (0.5%)
Haemorrhage	2 (4.0%)	26 (12.9%)
Normal study	13 (26.0%)	35 (17.4%)
Inconclusive	0	1 (0.5%)
Others <sup>†</sup>	7 (14.0%)	17 (8.5%)

\* Data are shown as No. (%).

<sup>†</sup> Air, morning glory syndrome, lymphocytic hypophysitis, syringomyelia, von Hippel–Lindau syndrome, Chiari malformation, extracranial mass, Parry-Romberg syndrome, and colpocephaly.

**Table 2.** Number of patients in which susceptibility-weighted imaging influenced detection rate and/or reported results.\*

Diagnosis	Influence on detection		Influence on reported results	
	Radiologist 1	Radiologist 2	Radiologist 1	Radiologist 2
Ischaemic stroke (n=10)	3 (30.0%)	3 (30.0%)	1 (10.0%)	0
Tumour (n=100)	59 (59.0%)	64 (64.0%)	6 (6.0%)	7 (7.0%)
Vascular disease (n=22)	22 (100%)	20 (90.9%)	20 (90.9%)	17 (77.3%)
Neurodegenerative / demyelinating disease (n=14)	11 (78.6%)	11 (78.6%)	10 (71.4%)	11 (78.6%)
Infection (n=2)	1 (50.0%)	2 (100%)	1 (50.0%)	0
Calcification (n=2)	2 (100%)	2 (100%)	0	0
Haemorrhage (n=28)	25 (89.3%)	25 (89.3%)	10 (35.7%)	8 (28.6%)
Normal study (n=48)	0	0	0	0
Inconclusive (n=1)	0	0	0	0
Others (n=24)†	5 (20.8%)	6 (25.0%)	1 (4.2%)	1 (4.2%)
Total (n=251)	128 (51.0%)	133 (53.0%)	49 (19.5%)	44 (17.5%)

\* Data are shown as No. (%).

† Air, morning glory syndrome, lymphocytic hypophysitis, syringomyelia, von Hippel-Lindau syndrome, Chiari malformation, extracranial mass, Parry-Romberg syndrome, and colpocephaly.

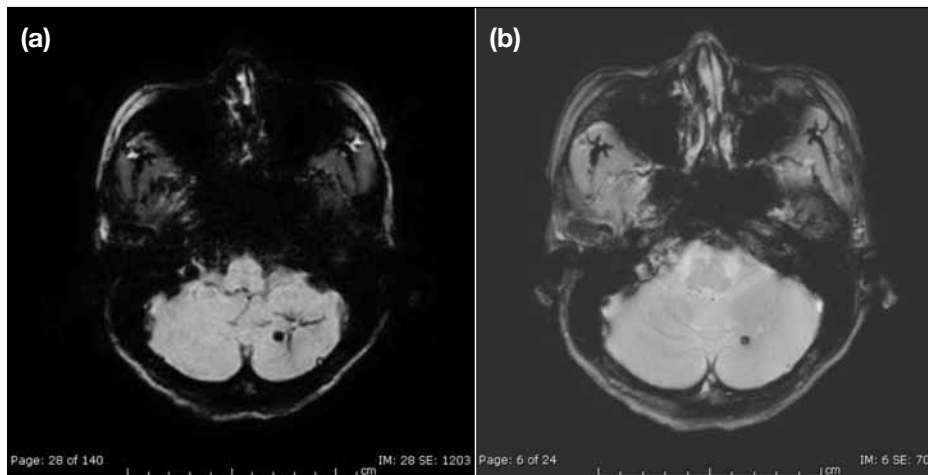


**Figure 1.** A 58-year-old woman presenting with ataxia. (a) Susceptibility-weighted imaging showing medusa-like hypointensity of developmental venous anomaly at the left cerebellar hemisphere, which was undetectable on gradient recalled echo T2-weighted image. (b) An adjacent cavernous malformation was seen.

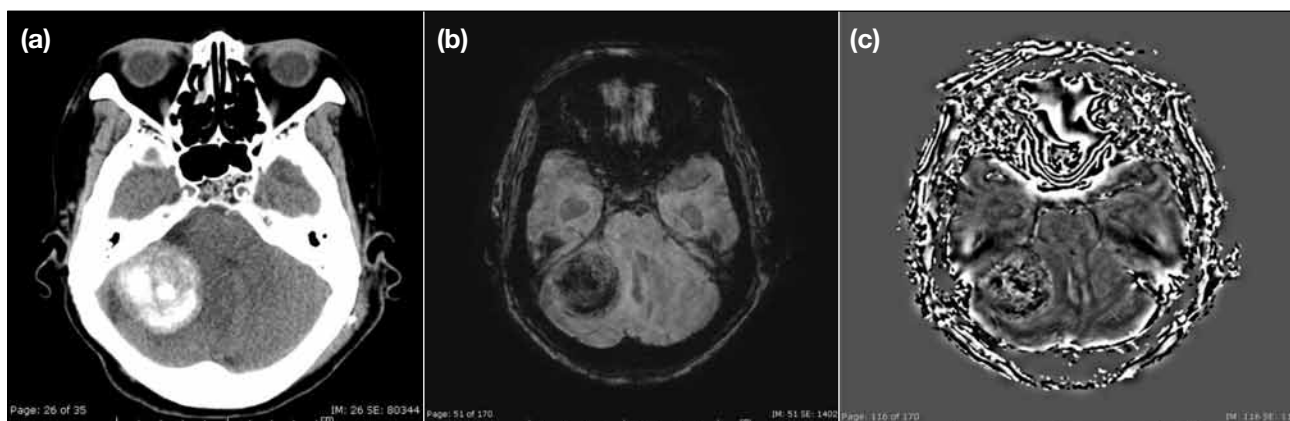


**Figure 2.** An 84-year-old woman presenting with alteration of consciousness. (a) Computed tomography scan showing calcified meningioma at right cerebellar convexity. (b, c) Magnitude and phase images of susceptibility-weighted imaging showing hypointensity corresponding to the areas of denser intratumoural calcification.

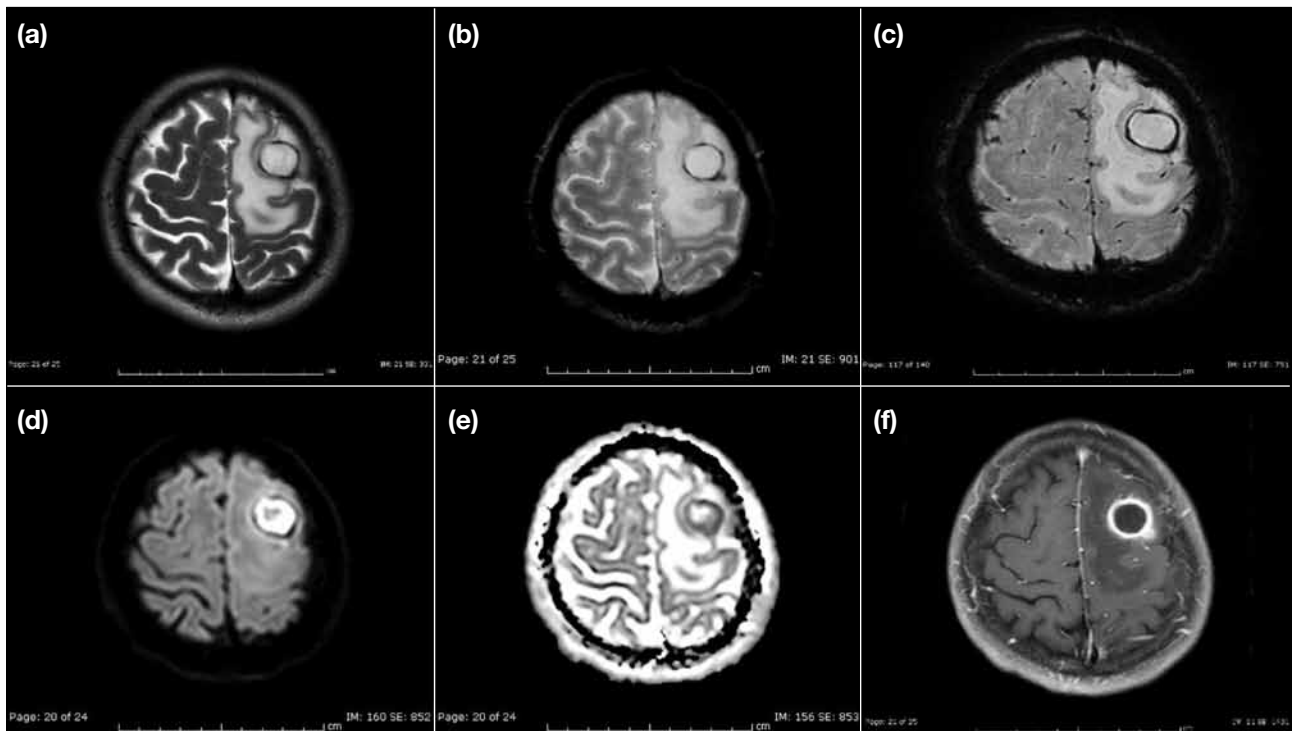


**Figure 3.** A 36-year-old woman presenting with fever and headache. (a) Axial T2-weighted image and (b) gradient recalled echo T2-weighted image showing a smooth thin hypointense rim. (c) Susceptibility-weighted imaging showing dual rim sign, defined as outer rim hypointensity and inner rim hyperintensity, a specific feature of pyogenic abscess. (d) Diffusion-weighted image and (e) apparent diffusion coefficient image showing restricted water diffusion. (f) Gadolinium-enhanced T1-weighted image showing smooth thin rim enhancement. Stereotactic biopsy found frank pus.

The detection rates and reported results for vascular disease were most strongly influenced by SWI in the present study. In particular, incidental findings of cavernous malformation, developmental venous anomaly, and capillary telangiectasia were influential. Similar to the results of Tsui et al,<sup>4</sup> Barnes et al,<sup>5</sup> and Tong et al,<sup>6</sup> SWI was better in demonstrating low-flow vascular malformations and had an improved detection rate. For high-flow vascular malformations such as arteriovenous malformation and dural arteriovenous fistula, both MinIP and MIP techniques can improve the image quality.<sup>7</sup> In the present study, SWI also demonstrated improvements in detection rates and diagnosis for abnormal venous structures in two patients with arteriovenous malformations that were in agreement with previous studies.<sup>8,9</sup> Our study is in agreement with a previous study that reported that SWI is a useful method to evaluate venous sinus thrombosis by demonstrating an increased deoxyhaemoglobin concentration in the area of venous stasis and collateral slow flows.<sup>10</sup>

Calcification cannot be differentiated from haemorrhage by a GRE image. Both cause local magnetic field

changes and appear as hypointensity. The phase image of SWI can distinguish these lesions; calcification is diamagnetic, whereas haemorrhage is paramagnetic, resulting in opposite signal intensities. The detection rate of SWI for intracranial calcification has previously been reported as 98.2%, which was significantly higher than T1W and T2W images.<sup>11</sup> This was not significantly different from the detection rate for calcification in the present study (100%, n=2) [Table 2].

The present study also agreed with another study that reported SWI is more sensitive than T1W and T2W images in identifying chronic haemorrhagic lesions and cerebral microbleeds.<sup>11</sup> However, few of our patients were affected by these diagnostic results.

A recent study reported that the dual rim sign is the most specific imaging feature differentiating pyogenic brain abscess from necrotic glioblastoma on SWI.<sup>12</sup> The outer hypointense rim corresponds to the enhanced abscess capsule, with production of paramagnetic free radicals caused by macrophages. The inner hyperintense rim is granulation tissue between the abscess cavity and

fibrocollagenous capsule. This dual rim sign was seen in two patients in the present study who were finally diagnosed as having pyogenic abscess.

Abnormally elevated iron levels are evident in many neurodegenerative disorders, including Parkinson's disease, Alzheimer's disease, Huntington's disease, and amyotrophic lateral sclerosis. However, iron deposition is commonly seen with increasing age.<sup>13,14</sup> It is more difficult to differentiate normal and pathologic mineralisation with advanced age because physiologic deposition such as calcium and iron are more pronounced in older patients. Comparison with age-matched SWI images can be helpful. SWI filtered phase imaging is suitable for demonstration of increased iron content and shows a better distinction between the pars compacta and the pars reticulata of the substantia nigra, which contains iron. In idiopathic Parkinson's disease, there is evidence of increased iron in the substantia nigra. SWI is a potentially useful imaging tool to identify iron deposition as a biomarker for disease progression. Accurate localisation of the subthalamic nucleus can be achieved on SWI, allowing safe direct targeting for placement of electrodes in the treatment of Parkinson's disease.<sup>15</sup> In patients with multiple sclerosis, very high iron deposition is seen in deep grey matter structures such as the pulvinar, caudate nucleus, putamen, and thalamus. Iron is also seen in the ring-like structures around some multiple sclerosis lesions that are often visible on SWI but not in conventional images.<sup>13,14,16</sup> In 8 of 12 patients with Parkinson's disease and one patient with multiple sclerosis, phase images were potentially helpful to detect and diagnose the diseases, but iron deposition was poorly seen or not visible on conventional MRI. Therefore, SWI should be performed in cases of neurodegenerative and demyelinating diseases, especially Parkinson's disease and multiple sclerosis. However, clinical correlation is important for diagnosis, because iron deposition is also part of the normal ageing process.

SWI can demonstrate internal characteristics of brain tumours including haemorrhage, neovascularity, calcification, and cystic component. It improves detection rates of tumour-related haemorrhage compared with GRE.<sup>17,18</sup> High-graded tumours such as glioblastoma often have a haemorrhagic component, which may be useful for staging. Kim et al<sup>19</sup> assessed the added value provided by SWI in the differential diagnosis of solitary enhancing brain lesions compared with conventional MRI alone. Preoperative SWI evaluation of a butterfly mass in the present study revealed multiple haemorrhagic

foci on SWI; therefore, they were differentiated from lymphoma and ultimately diagnosed as glioblastoma. However, most patients in the present study came for interval follow-up after treatment for brain tumours, including surgery and radiation therapy. Post-treatment SWI detected haemorrhage and microbleeds more often than did conventional MRI; however, this did not influence the reported results.

Several studies have reported that SWI is more sensitive in detecting haemorrhage within an infarct than CT and T2\*-weighted imaging or GRE scans.<sup>20-22</sup> Furthermore, SWI can detect haemorrhagic transformation earlier than CT.<sup>13,17,20,21,23</sup> SWI is also helpful for monitoring complications after revascularisation therapy. Decreased arterial blood oxygenation causes increased deoxyhaemoglobin in the infarcted area; the increased hypointensity along the affected cortex is detected on T2\*-weighted imaging, and both magnitude and phase images of SWI.<sup>24</sup> The difference between arterial and venous vessels cannot be seen with conventional MRI sequences. Prominent veins within areas of impaired perfusion allow the identification of penumbral brain tissue. In 3 of 10 patients with stroke in the present study, haemorrhage and microbleeds were more distinctive in the infarcted area on SWI than on conventional MRI. In one of these patients, SWI revealed transmedullary veins that were not seen on conventional MRI.

Our study had a few limitations. First, despite the large number of patients, they were not proportionately distributed in each group. Second, the final diagnosis was made by various methods, including pathological results in cases of surgery, comparison with previous studies or interval follow-up, and by consensus of the two neuroradiologists.

## CONCLUSION

SWI is a helpful technique on routine brain MRI that has an influence on detection rates and reported results, especially for vascular diseases, microbleeds, infection, neurodegenerative / demyelinating disease, and evaluation of intratumoural components. It is recommended that SWI should be added to conventional MRI sequences.

## REFERENCES

1. Haacke EM, Mittal S, Wu Z, Neelavalli J, Cheng YC. Susceptibility-weighted imaging: technical aspects and clinical applications, part 1. *AJNR Am J Neuroradiol*. 2009;30:19-30. [Crossref](#)
2. Reichenbach JR, Venkatesan R, Schillinger DJ, Kido DK,

- Haacke EM. Small vessels in the human brain: MR venography with deoxyhemoglobin as an intrinsic contrast agent. *Radiology*. 1997;204:272-7. [Crossref](#)
3. Rauscher A, Sedlacik J, Barth M, Mentzel HJ, Reichenbach JR. Magnetic susceptibility-weighted MR phase imaging of the human brain. *AJNR Am J Neuroradiol*. 2005;26:736-42.
  4. Tsui YK, Tsai FY, Hasso AN, Greensite F, Nguyen BV. Susceptibility-weighted imaging for differential diagnosis of cerebral vascular pathology: a pictorial review. *J Neurol Sci*. 2009;287:7-16. [Crossref](#)
  5. Barnes SR, Haacke EM. Susceptibility-weighted imaging: clinical angiographic applications. *Magn Reson Imaging Clin N Am*. 2009;17:47-61. [Crossref](#)
  6. Tong KA, Ashwal S, Holshouser BA, Nickerson JP, Wall CJ, Shutter LA, et al. Diffuse axonal injury in children: clinical correlation with hemorrhagic lesions. *Ann Neurol*. 2004;56:36-50. [Crossref](#)
  7. Jagadeesan BD, Delgado Almandoz JE, Moran CJ, Benzinger TL. Accuracy of susceptibility-weighted imaging for the detection of arteriovenous shunting in vascular malformations of the brain. *Stroke*. 2011;42:87-92. [Crossref](#)
  8. Juhász C, Haacke EM, Hu J, Xuan Y, Makki M, Behen ME, et al. Multimodality imaging of cortical and white matter abnormalities in Sturge-Weber syndrome. *AJNR Am J Neuroradiol*. 2007;28:900-6.
  9. Hu J, Yu Y, Juhasz C, Kou Z, Xuan Y, Latif Z, et al. MR susceptibility weighted imaging (SWI) complements conventional contrast enhanced T1 weighted MRI in characterizing brain abnormalities of Sturge-Weber syndrome. *J Magn Reson Imaging*. 2008;28:300-7. [Crossref](#)
  10. Hinman JM, Provenzale JM. Hypointense thrombus on T2-weighted MR imaging: a potential pitfall in the diagnosis of dural sinus thrombosis. *Eur J Radiol*. 2002;41:147-52. [Crossref](#)
  11. Zhu WZ, Qi JP, Zhan CJ, Shu HG, Zhang L, Wang CY, et al. Magnetic resonance susceptibility weighted imaging in detecting intracranial calcification and hemorrhage. *Chin Med J (Engl)*. 2008;121:2021-5. [Crossref](#)
  12. Toh CH, Wei KC, Chang CN, Hsu PW, Wong HF, Ng SH, et al. Differentiation of pyogenic brain abscesses from necrotic glioblastomas with use of susceptibility-weighted imaging. *ANJR Am J Neuroradiol*. 2012;33:1534-8. [Crossref](#)
  13. Thomas B, Somasundaram S, Thamburaj K, Kesavadas C, Gupta AK, Bodhey NK, et al. Clinical applications of susceptibility weighted MR imaging of the brain—a pictorial review. *Neuroradiology*. 2008;50:105-16. [Crossref](#)
  14. Haacke EM, Xu Y, Cheng YC, Reichenbach JR. Susceptibility-weighted imaging (SWI). *Magn Reson Med*. 2004;52:612-8. [Crossref](#)
  15. Vertinsky AT, Coenen VA, Lang DJ, Kolind S, Honey CR, Li D, et al. Localization of the subthalamic nucleus: optimization with susceptibility-weighted phase MR imaging. *AJNR Am J Neuroradiol*. 2009;30:1717-24. [Crossref](#)
  16. Haacke EM, Ayaz M, Khan A, Manova ES, Krishnamurthy B, Gollapalli L, et al. Establishing a baseline phase behavior in magnetic resonance imaging to determine normal vs. abnormal iron content in the brain. *J Magn Reson Imaging*. 2007;26:256-64. [Crossref](#)
  17. Sehgal V, Delproposto Z, Haacke EM, Tong KA, Wycliffe N, Kido DK, et al. Clinical applications of neuroimaging with susceptibility-weighted imaging. *J Magn Reson Imaging*. 2005;22:439-50. [Crossref](#)
  18. Sehgal V, Delproposto Z, Hadder D, Haacke EM, Sloan AE, Zamorano LJ, et al. Susceptibility-weighted imaging to visualize blood products and improve tumor contrast in the study of brain masses. *J Magn Reson Imaging*. 2006;24:41-51. [Crossref](#)
  19. Kim HS, Jahng GH, Ryu CW, Kim SY. Added value and diagnostic performance of intratumoral susceptibility signals in the differential diagnosis of solitary enhancing brain lesions: preliminary study. *AJNR Am J Neuroradiol*. 2009;30:1574-9. [Crossref](#)
  20. Wycliffe ND, Choe J, Holshouser B, Oyoyo UE, Haacke EM, Kido DK. Reliability in detection of hemorrhage in acute stroke by a new three-dimensional gradient recalled echo susceptibility-weighted imaging technique compared to computed tomography: a retrospective study. *J Magn Reson Imaging*. 2004;20:372-7. [Crossref](#)
  21. Santhosh K, Kesavadas C, Thomas B, Gupta AK, Thamburaj K, Kapilamoorthy TR. Susceptibility weighted imaging: a new tool in magnetic resonance imaging of stroke. *Clin Radiol*. 2009;64:74-83. [Crossref](#)
  22. Nighoghossian N, Hermier M, Adeleine P, Blanc-Lasserre K, Derex L, Honnorat J, et al. Old microbleeds are a potential risk factor for cerebral bleeding after ischemic stroke: a gradient-echo T2\*-weighted brain MRI study. *Stroke*. 2002;33:735-42. [Crossref](#)
  23. Hermier M, Nighoghossian N. Contribution of susceptibility-weighted imaging to acute stroke assessment. *Stroke*. 2004;35:1989-94. [Crossref](#)
  24. Tamura H, Hatazawa J, Toyoshima H, Shimosegawa E, Okudera T. Detection of deoxygenation-related signal change in acute ischemic stroke patients by T2\* weighted magnetic resonance imaging. *Stroke*. 2002;33:967-71. [Crossref](#)